Electroluminescence and photovoltaic properties of poly(p-phenylene vinylene) derivatives with dendritic pendants

ARTICLE *in* JOURNAL OF APPLIED POLYMER SCIENCE · JANUARY 2008

Impact Factor: 1.77 · DOI: 10.1002/app.27119

7 AUTHORS, INCLUDING:

Zhan'ao Tan
North China Electric Power University
88 PUBLICATIONS **3,464** CITATIONS
SEE PROFILE

Erjun Zhou
National Center for Nanoscience and Technology
46 PUBLICATIONS **2,113** CITATIONS
SEE PROFILE

fu xi
Technical Institute of Physics and Chemistry
102 PUBLICATIONS **2,055** CITATIONS
SEE PROFILE

Electroluminescence and Photovoltaic Properties of Poly(*p*-phenylene vinylene) Derivatives with Dendritic Pendants

Zhan'ao Tan,[1,2] Rupei Tang,[3,4] Erjun Zhou,[1,2] Youjun He,[1] Chunhe Yang,[1] Fu Xi,[4] Yongfang Li[1]

[1]*Beijing National Laboratory for Molecular Sciences, Key Laboratory of Organic Solids, Institute of Chemistry, Chinese Academy of Sciences, Beijing 100080, China*
[2]*Graduate School, Chinese Academy of Sciences, Beijing 100039, China*
[3]*Department of Chemical Engineering, Wuhan University of Technology, Wuhan 430070, China*
[4]*State Key Laboratory of Polymer Physics and Chemistry, Joint Laboratory of Polymer Science and Materials, Institute of Chemistry, Chinese Academy of Sciences, Beijing 100080, China*

Received 24 September 2006; accepted 18 June 2007
DOI 10.1002/app.27119
Published online 21 September 2007 in Wiley InterScience (www.interscience.wiley.com).

ABSTRACT: A copolymer of dendronized poly(*p*-phenylene vinylene) (PPV), poly{2-[3′,5′-bis (2′-ethylhexyloxy) bnenzyloxy]-1,4-phenylene vinylene}-co-poly[2-methoxy-5-(2′-ethylhexyloxy)-1,4-phenylene vinylene] (BE-*co*-MEH–PPV), was synthesized with the Gilch route to improve the electroluminescence and photovoltaic properties of the dendronized PPV homopolymer. The polymer was characterized by ultraviolet–visible absorption spectroscopy, photoluminescence spectroscopy, and electrochemical cyclic voltammetry and compared with the homopolymers poly{2-[3′, 5′-bis(2-ethylhexyloxy) benzyloxy-1,4-phenylene vinylene} (BE–PPV) and poly[2-methoxy-5-(2′-ethylhexyloxy)-1,4-phenylenevinylene] (MEH–PPV). Polymer light-emitting diodes based on the polymers with the configuration of indium tin oxide (ITO)/poly(3,4-ethylene dioxythiophene) : poly(styrene sulfonate) (PEDOT : PSS)/polymer/Ca/Al were fabricated. The electroluminescence efficiency of BE-*co*-MEH–PPV reached 1.64 cd/A, which was much higher than that of BE–PPV (0.68 cd/A) and a little higher than that of MEH–PPV (1.59 cd/A). Photovoltaic properties of the polymer were studied with the device configuration of ITO/PEDOT : PSS/polymer : [6,6J-phenyl-C_{61}-butyric acid methyl ester] (PCBM)/Mg/Al. The power conversion efficiency of the device based on the blend of BE-*co*-MEH–PPV and PCBM with a weight ratio of 1 : 3 reached 1.41% under the illumination of air mass 1.5 (AM1.5) (80 mW/cm^2), and this was an improvement in comparison with 0.24% for BE–PPV and 1.32% for MEH–PPV under the same experimental conditions. © 2007 Wiley Periodicals, Inc. J Appl Polym Sci 107: 514–521, 2008

Key words: block copolymers; conjugated polymers; light-emitting diodes (LED); photophysics

INTRODUCTION

Solution-processable conjugated polymers have attracted much attention because of their applications in developing low-cost optoelectronic devices, such as polymer light-emitting devices,[1,2] polymer solar cells (PSCs),[3,4] and thin-film transistors.[5] Conjugated polymers are particularly versatile because of the feasible design of the molecular structures and easy modification of their physical properties (absorption and photoluminescent properties).[6] As one of the most important conjugated polymers, poly(*p*-phenylene vinylene) (PPV) and its derivatives are widely employed as active materials in polymer light-emitting diodes (PLEDs) and photovoltaic cells.[7,8] Generally, bulky substituents such as alkoxy, alkylsilyl, phenyl, and fluorenyl groups are introduced into the PPV backbone to modify the chemical structure and fine-tune the luminescent properties.[9–12]

Recently, Tang and coworkers[13,14] reported the synthesis, electroluminescence (EL), and photovoltaic properties of PPV homopolymers bearing various dendritic side chains by the Gilch route.[15] The introduction of bulky dendritic pendants into PPVs could effectively suppress intermolecular interactions such as aggregation and excimer formation.[16–18] However, relatively low EL and photovoltaic efficiencies of the dendronized polymers were observed,[13] probably because of the more twisted conformation of the polymers with the large dendritic side groups. Copolymerization of different monomers is frequently used to prepare functional polymers. For the PPV-based PLEDs and PSCs, poly[2-methoxy-5-(2′-ethylhexyloxy)-1,4-phenylenevinylene] (MEH–PPV) has been one of the most widely studied active materials because of its better optoelectronic performance.[2,19,20]

Correspondence to: F. Xi (xifu@iccas.ac.cn) or Y. Li (liyf@iccas.ac.cn)

Contract grant sponsor: Ministry of Science and Technology of China through the 973 Project; contract grant number: 2002CB613404.

Contract grant sponsor: National Natural Science Foundation of China; contract grant numbers: 50273042, 20474069, 20421101, 20574078, and 50633050.

Journal of Applied Polymer Science, Vol. 107, 514–521 (2008)

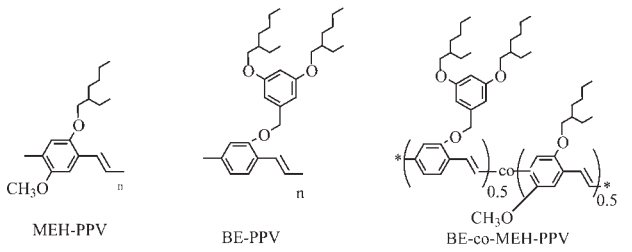

Figure 1 Molecular structures of MEH–PPV and PPV derivatives bearing dendritic pendants.

To improve the EL and photovoltaic performance of the dendronized PPVs, we herein synthesized a dendronized PPV copolymer with MEH–PPV by the Gilch route, and its EL and photovoltaic properties were improved obviously in comparison with those of the homopolymers poly{2-[3′,5′-bis(2-ethylhexyloxy) benzyloxy]-1,4-phenylene vinylene} (BE–PPV) and MEH–PPV (the molecular structures of the polymers are shown in Fig. 1).

EXPERIMENTAL

Measurements

^{1}H-NMR spectra were recorded with a Bruker AM-300 spectrometer (Karlsruhe, Germany), and chemical shifts were recorded in parts per million. The molecular weights and polydispersity index (PDI) of the polymers were determined by gel permeation chromatography analysis [a Waters 515 high performance liquid chromatography pump, a Waters 2414 differential refractometer, and three Waters Styragel columns (HT2, HT3, and HT4)] with tetrahydrofuran (THF) as an eluent at a flow rate of 1.0 mL/min at 35°C and with polystyrene as a standard. Thermogravimetric analysis (TGA) was conducted on a Perkin Elmer 7 thermogravimetric analyzer at a heating rate of 20°C/min under a nitrogen atmosphere. Ultraviolet–visible (UV–vis) spectra were recorded on a Hitachi UV-3010 spectrometer (Japan). Photoluminescence (PL) and EL spectra were obtained with a Hitachi F-4500 fluorescence spectrophotometer. Electrochemical cyclic voltammetry was conducted on a Zahner IM6e electrochemical workstation (Germany) with a Pt disk, a Pt plate, and Ag/Ag^+ as a working electrode, a counter electrode, and a reference electrode, respectively, in a 0.1*M* tetrabutylammonium hexafluorophosphate (Bu_4NPF_6) acetonitrile solution. Current–voltage and light intensity–voltage characteristics of the polymer light-emitting devices were recorded with a computer-controlled Keithley (United States) 236 source measure unit and a Keithley 2000 multimeter coupled with a Si photomultiplier tube. The current–voltage measurements of PSCs were conducted on a computer-controlled Keithley 236 source measure unit. A xenon lamp simulated a white-light source; the optical power at the sample was 80 mW/cm^2. All the measurements were performed under the ambient atmosphere at room temperature.

Materials

THF was distilled over sodium and benzophenone. All other solvents and reagents were analytical-grade quality, were purchased commercially, and were used without further purification.

Synthesis

The synthetic route of poly{2-[3′,5′-bis(2′-ethylhexyloxy)benzyloxy]-1,4-phenylene vinylene}-co-poly[2-methoxy-5-(2′-ethylhexyloxy)-1,4-phenylene vinylene] (BE-*co*-MEH–PPV) is shown in Scheme 1. The preparation of 2-(3′,5′-bis(2″-ethylhexyloxy)benzyloxy)-1,4-bis(bromomethyl)benzene (**1**) was previously reported.[13,14] 2-Methoxy-5-(2′-ethylhexyloxy)-1,4-bis (bromomethyl)benzene (**2**) was prepared according to a literature procedure.[21]

BE-*co*-MEH–PPV

To a stirred solution of **1** (0.20 g, 0.32 mmol) and **2** (0.13 g, 0.32 mmol) in dry THF (40 mL) under argon at room temperature was added dropwise potassium *tert*-butoxide (3.8 mL, 1.0 mol/L in THF, 3.80 mmol). The mixture was stirred overnight at room temperature. The viscous mixture was added dropwise to stirred methanol. The crude polymer was collected by filtration, washed with methanol, and stirred with two portions of a mixture of methanol and water (1/1) for 1 h. The polymer was filtered off, washed with methanol, dried under a high vacuum, and dissolved in chloroform. The solution was filtered, and the polymer was precipitated by dropwise addition to methanol. The precipitated polymer was

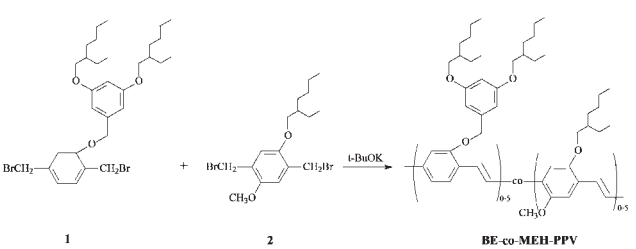

Scheme 1 Synthetic route of BE-*co*-MEH–PPV.

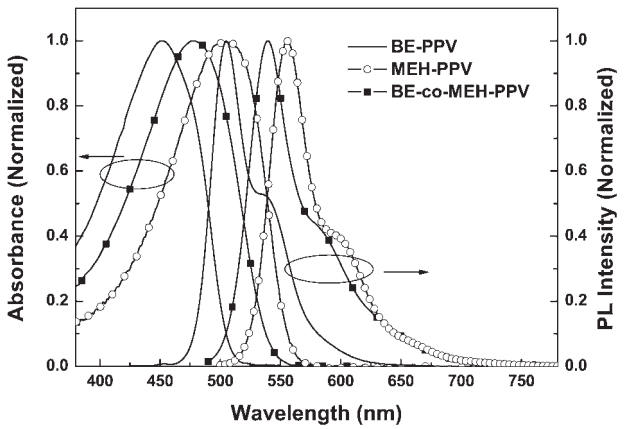

Figure 2 Absorption and PL spectra of the polymer solutions in chloroform.

collected, washed with methanol, and dried *in vacuo*. Then, the polymer was again dissolved in chloroform, filtered, precipitated with methanol, and dried *in vacuo* to yield 145 mg of a red solid.

Yield: 63%. Number-average molecular weight = 110 K. PDI = 1.64. TGA: 345°C. ^{1}H-NMR ($CDCl_3$, 400 MHz, δ/ppm): 7.53(br, 4H, Ar—H), 7.24–7.00 (br, 5H, Ar—H, CH=CH), 6.65 (s, 2H, Ar—H), 6.41 (s, 1H, Ar—H), 5.15 (br, 2H, Ar—CH_2), 3.97–3.73 (br, 9H, OCH_2, OCH_3), 1.86–1.25 (br, 27H, CH, CH_2), 0.90–0.84 (br, 18H, CH_3). ANAL. CALCD. for $(C_{31}H_{44}O_3)_{0.5}$ $(C_{17}H_{24}O_2)_{0.5}$: C, 79.51%; H, 9.45%; O, 11.03%. Found: C, 78.76%; H, 9.52%.

RESULTS AND DISCUSSION

Synthesis and structural characterization of the two copolymers

BE-*co*-MEH–PPV was prepared with the Gilch polymerization method,[15] as shown in Scheme 1. During the polymerization, the reaction mixture remained homogeneous without any formation of gel portions, gradually became viscous, and showed strong fluorescence. The synthesized copolymers were easily dissolved in common organic solvents, such as chloroform, toluene, and xylene, at room temperature. The structure of the copolymer was identified by ^{1}H-NMR spectroscopy. The benzyl proton peaks at about 4.50 ppm for monomers disappeared after the polymerization, and new vinyl proton peaks at about 7.0–7.2 ppm together with phenyl protons appeared, confirming the polymerization reaction. The weight-average molecular weights of BE-*co*-MEH–PPV, BE–PPV, and MEH–PPV were 1.81×10^5, 2.16×10^5, and 2.35×10^5 with PDIs of 1.64, 1.53, and 1.48, respectively.

The TGA curve of the polymer revealed a relatively high thermal stability, and the initial weight loss (5%) temperature of BE-*co*-MEH–PPV was found to be about 345°C.

Optical properties

Figure 2 shows the optical absorption and PL spectra of BE–PPV, MEH–PPV, and BE-*co*-MEH–PPV in dilute chloroform solutions. BE–PPV has an absorption maximum at about 452 nm, and the maximum absorption of MEH–PPV is at about 502 nm. As expected, the absorption spectrum of the BE-*co*-MEH–PPV copolymer, with maximum absorption at about 479 nm, broadened and redshifted in comparison with that of BE–PPV, whereas it blueshifted in comparison with that of MEH–PPV. The absorptions are attributed to the π–π* transition of the main chains of the conjugated polymers. The broadened and redshifted absorption band indicates a lower π–π* transition energy or a narrower band gap of the copolymer in comparison with that of BE–PPV, which could be attributed to the extended conjugation system of the polymer benefiting from the coplanarity of the polymer main chains. In a dilute chloroform solution, BE–PPV emits green light, whereas BE-*co*-MEH–PPV emits orange light. As shown in Figure 2, the maximum emissions of BE–PPV, MEH–PPVs and BE-*co*-MEH–PPV in dilute chloroform solutions were observed at about 506, 555, and 540 nm, respectively.

Figure 3 shows the absorption and PL spectra of BE–PPV, MEH–PPV, and BE-*co*-MEH–PPV in solid films. The absorption bands of the polymer films are broadened and redshifted in comparison with the solution spectra. The results suggest a significant increase in the conjugation length in the solid state, and this is mostly due to the more planar conformation resulting from π-stacking/aggregation in the solid state. The maximum absorption of BE–PPV and MEH–PPV films is at 470 and 515 nm, respectively,

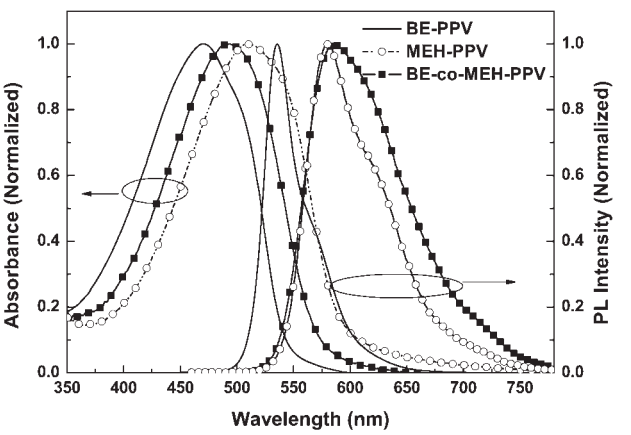

Figure 3 UV–vis absorption and PL spectra of the polymer films.

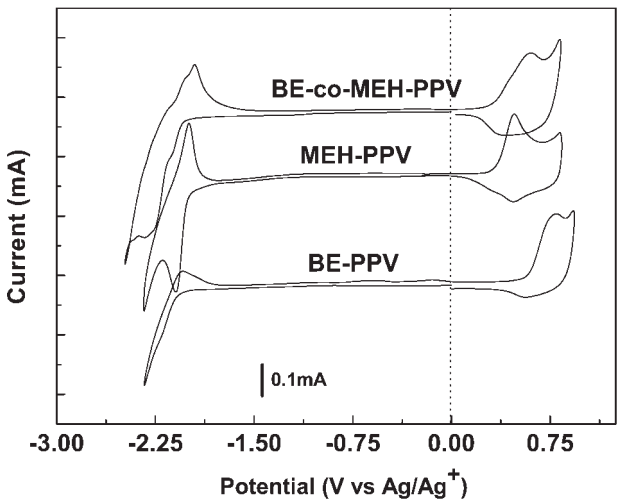

Figure 4 Cyclic voltammograms of the polymer films in a 0.1 mol/L Bu_4NPF_6 acetonitrile solution (scan rate = 20 mV/s).

and the maximum absorption of the BE-*co*-MEH–PPV film is at 494 nm. Compared with the solution PL spectra, the PL spectra of the polymer films are redshifted by about 30–40 nm. The PL peak of the BE-*co*-MEH–PPV film is at about 586 nm. Interestingly, the PL peak of the BE-*co*-MEH–PPV film is a little redshifted from that of the MEH–PPV film, whereas that of the copolymer solution is blueshifted in comparison with that of the MEH–PPV solution. The interplane interaction of the polymer main chains in the copolymer is probably stronger than that of MEH–PPV.

Electrochemical properties

Electrochemical cyclic voltammetry is often performed for determining the energy levels of the highest occupied molecular orbital (HOMO) and lowest unoccupied molecular orbital (LUMO) of conjugated polymers.[22] Figure 4 shows the cyclic voltammograms of the dendritic PPV films on a Pt electrode in a 0.1 mol/L Bu_4NPF_6, acetonitrile solution. It can be seen that there are electrochemically quasi-reversible *p*-doping/dedoping processes in a positive potential range and *n*-doping/dedoping processes in a negative potential range for all the polymers. From the onset oxidation potential (E_{ox}) and onset reduction potential (E_{red}) values of the polymers, HOMO and LUMO energy levels as well as the energy gap (E_g^{ec}) of the polymers were calculated according to the following equations:[23]

$$\text{HOMO (eV)} = -(E_{ox} + 4.71)$$

$$\text{LUMO (eV)} = -(E_{red} + 4.71)$$

$$E_g^{ec} = e(E_{ox} - E_{red})$$

where the units of *E*ox and *E*red are volts versus Ag/Ag^+. The obtained values are listed in Table I. In comparison with BE–PPV, the onset *p*-doping (oxidation) potential (ca. 0.3 V vs Ag/Ag^+) of BE-*co*-MEH–PPV is more than 0.2 V lower, and the onset *n*-doping (reduction) potential decreases only a little. Obviously, the band-gap reduction (corresponding to the redshift of the absorption) mainly resulted from the increase in HOMO of the copolymer. The results mean that the copolymer more easily yielded electrons; that is, the donor ability increased for the copolymer.

EL properties

Single-layer PLED devices based on dendronized PPVs and MEH–PPV with the configuration of indium tin oxide (ITO)/poly(3,4-ethylene dioxythiophene) : poly(styrene sulfonate) (PEDOT : PSS; 30 nm)/polymer (80 nm)/Ca (10 nm)/Al (150 nm) were fabricated. A poly(3,4-ethylene dioxythiophene) (PEDOT) layer was spin-cast onto a precleaned ITO substrate and was dried subsequently at 80°C in a vacuum oven. The polymer film was spin-coated from its toluene solution (10 mg/mL, 2500 rpm) onto the ITO/PEDOT : PSS film and dried at 80°C for 30 min. After that, the Ca cathode was thermally evaporated under a vacuum of less than 5×10^{-5} Pa. The cathode layer was coated with an Al layer by thermal evaporation to improve the stability of the devices in air.

The EL spectra of the devices are displayed in Figure 5. The PLED based on BE–PPV emitted yellow-green light, and the device based on BE-*co*-MEH–PPV and MEH–PPV emitted reddish-orange light. The EL peaks of BE–PPV, MEH–PPV, and BE-*co*-MEH–PPV were almost identical to those of their PL spectra shown in Figure 3, and this indicated that the PL and EL processes experienced the same excited state.

Figure 6 shows current density–voltage and luminance–voltage characteristics of the PLED devices. The turn-on voltages of the PLEDs based on BE–PPV and BE-*co*-MEH–PPV were approximately 5 and 4.4 V, respectively, which were lower than those of other PPV dendrimers.[24,25] As shown in Figure

TABLE I
Cyclic Voltammetry Results for the Polymer Films

Polymer	E_{red} (V)	E_{ox} (V)	LUMO (eV)	HOMO (eV)	E_g^{ec} (eV)
BE–PPV	−2.04	0.57	−2.68	−5.28	2.61
MEH–PPV	−1.90	0.30	−2.80	−5.01	2.21
BE-*co*-MEH–PPV	−2.02	0.31	−2.69	−5.02	2.33

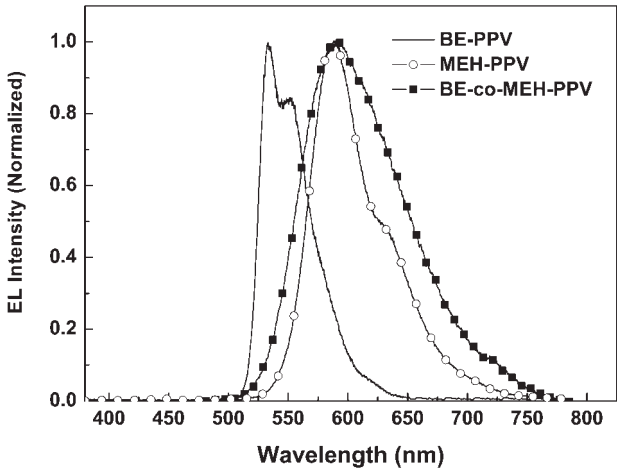

Figure 5 EL spectra of the ITO/PEDOT : PSS/polymer/Ca/Al PLEDs.

6(b), the maximum luminance of the single-layer PLEDs based on BE–PPV was about 523 cd/m^2 at 13 V. The maximum luminance of BE-*co*-MEH–PPV was about 3988 cd/m^2 at 15 V, which was more than 7 times higher than that of BE–PPV.

As shown in Figure 7, the maximum EL efficiency of the devices based on BE-*co*-MEH–PPV was 1.64 cd/A, which was almost 3 times higher than that of BE–PPV (0.68 cd/A). The maximum EL efficiency of BE-*co*-MEH–PPV was slightly enhanced compared with that (1.59 cd/A) of MEH–PPV. The dramatically enhanced performance of BE-*co*-MEH–PPV was probably attributable to the efficient intramolecular energy transfer in the copolymer system. The EL properties and Commission Internationale de l'Eclairage (CIE) chromaticity coordinates (x, y) at maximum luminance of the PLEDs based on the polymers are summarized in Table II.

The lower EL efficiency and maximum luminance of BE–PPV are probably due to the poor charge carrier injection and transportation of the polymer because of its larger side groups.[13,14] Figure 8 shows the electronic energy levels of the polymers and the work function of the electrodes in the PLEDs. For BE–PPV, there are about 0.2-eV electron injection barriers at the Ca/polymer interface and about 0.3-eV hole injection barriers at the PEDOT/polymer interface. As for BE-*co*-MEH–PPV, there is little hole injection barrier at the anode interface, and there is only a 0.1-eV electron injection barrier at the cathode interface. Thus, the turn-on voltage of the PLED based on BE-*co*-MEH–PPV is lower than that of BE–PPV, and the overall performance of the copolymer is expected to be better than that of the homopolymer BE–PPV.

Photovoltaic properties

PSCs were fabricated with the configuration of ITO/PEDOT : PSS (30 nm)/polymer:PCBM blend (80 nm)/

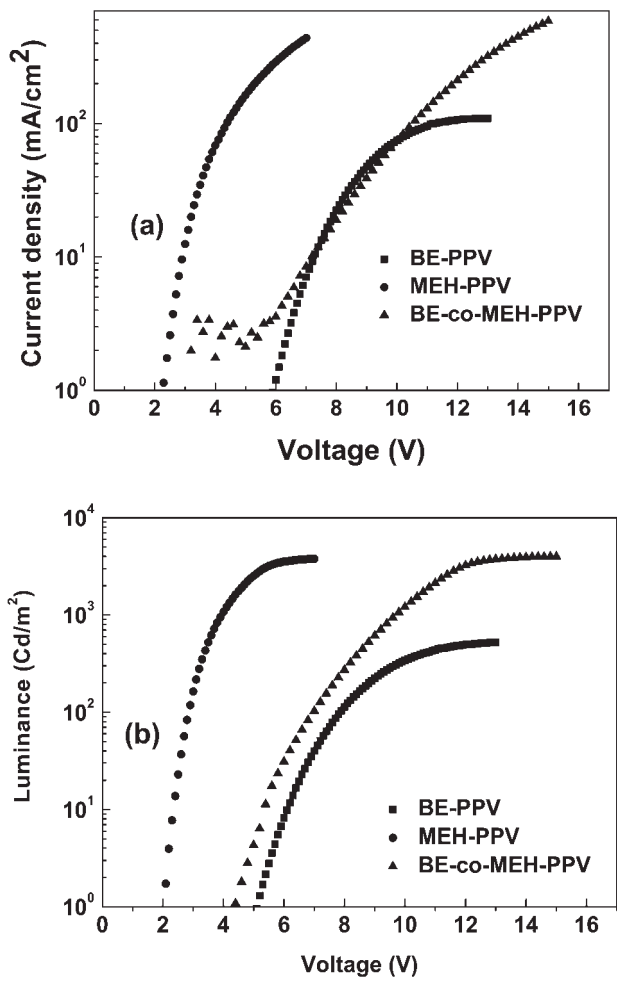

Figure 6 (a) Current density–voltage and (b) luminance–voltage curves of the PLEDs.

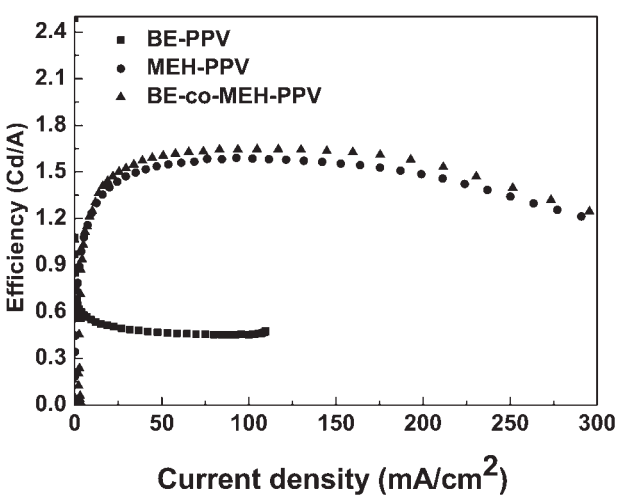

Figure 7 EL current efficiency of the single-layer PLEDs based on the polymers.

TABLE II
Electroluminescent Properties of the PLEDs Based on the Polymers

Polymer	EL maximum wavelength (nm)	Turn-on voltage (V)	Luminance at maximum bias voltage (cd/m^2)/ voltage (V)	Maximum luminescence efficiency (cd/A)	CIE (x, y)
BE–PPV	540	5	523/13	0.68	0.33, 0.64
MEH–PPV	588	2	3788/7	1.59	0.60, 0.40
BE-*co*-MEH–PPV	586	4.4	3988/15	1.64	0.60, 0.40

Mg (10 nm)/Al (150 nm) for investigating the photovoltaic properties of the polymers. The photosensitive layer of the polymer/PCBM blend was prepared by the spin coating of a mixed solution of the polymer and PCBM in chlorobenzene and then dried at 80°C for 30 min. Finally, a magnesium/aluminum cathode was thermally deposited at a base pressure of 10^{-5} Pa. The blended film and the cathode were prepared inside dry nitrogen glove boxes without air exposure. Power conversion efficiency (η) values were measured under an air mass 1.5 (AM1.5) solar simulator with 80 mW/cm^2.

Figure 9 shows the current–voltage characteristics for the PSCs with various polymer/PCBM weight ratios made from BE–PPV, BE-*co*-MEH–PPV, and MEH–PPV. The relevant data for the photovoltaic properties of the PSCs are summarized in Table III.

As shown previously, the BE–PPV/PCBM (1 : 3 w/w) device had an open-circuit voltage (V_{oc}) of 0.75 V, a short-circuit current density (I_{sc}) of 0.63 mA/cm^2, and a fill factor (FF) of 41%; η of the device was calculated to be 0.24%. The lower photovoltaic performance of BE–PPV was probably due to the larger band gap with poor harvesting of the solar light. Figure 9 also shows the current–voltage characteristics based on BE-*co*-MEH–PPV for various PCBM concentrations. Obviously, with an increase in the PCBM concentration (the polymer/PCBM weight ratio changed from 1 : 2 to 1 : 3), V_{oc}, I_{sc}, FF, and η all increased. When the PCBM concentration reached 75 wt % (with a weight ratio of 1 : 3), BE-*co*-MEH–PPV exhibited the best photovoltaic property, and V_{oc}, I_{sc}, FF, and η reached 0.81 V, 3.37 mA/cm^2, 42%, and 1.41%, respectively. η was 5 times higher than that of BE–PPV-based devices and a little higher than that of the PSC based on MEH–PPV/PCBM (1 : 3) under the identical experimental conditions. The parameters of the PSC based on MEH–PPV/PCBM (1 : 3) were as follows: V_{oc} = 0.81 V, I_{sc} = 3.33 mA/cm^2, FF = 39%, and η = 1.32%. They were in accordance with previously reported results under the same conditions.[26,27]

When we further increased the concentration of PCBM to the weight ratio of 1 : 4, V_{oc}, I_{sc}, and FF of all the PSCs decreased, and consequently, η decreased. This was confirmed by the input photon to converted current efficiency (IPCE) of the device based on BE-*co*-MEH–PPV with different PCBM concentrations, as shown in Figure 10. With the weight ratios of the polymer to PCBM changing from 1 : 2 to 1 : 3 and then to 1 : 4, the IPCE value of BE-*co*-MEH–PPV at a 500-nm wavelength increased from 0.32 to 0.38 and then dropped to 0.21.

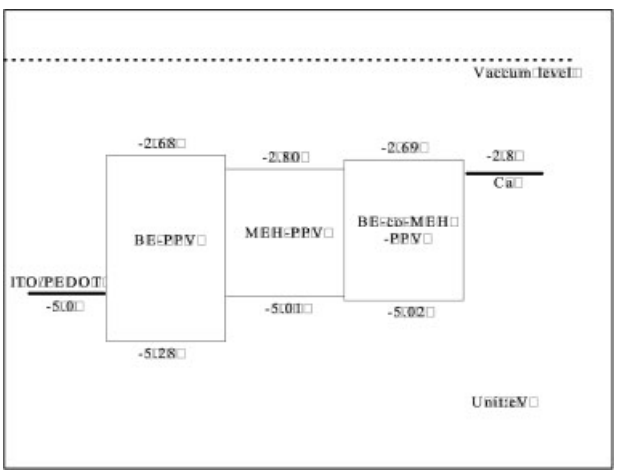

Figure 8 Electronic energy levels of the polymers and the work functions of the electrodes.

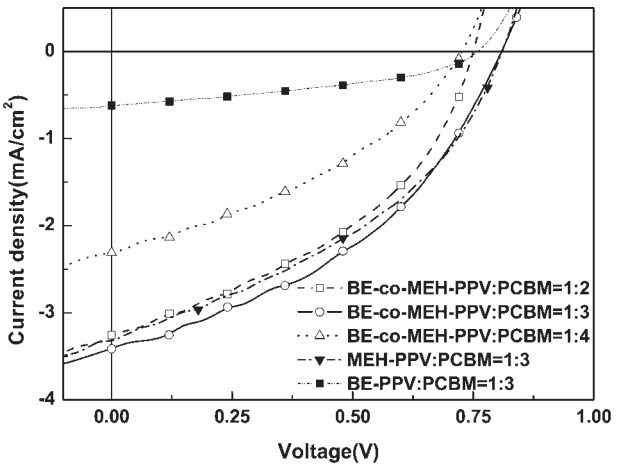

Figure 9 Current–voltage curves of the PSCs based on BE–PPV, MEH–PPV, and BE-*co*-MEH–PPV under the illumination of AM1.5 (80 mW/cm^2).

The effect of the PCBM concentration in the blend films on the photovoltaic properties could be explained as follows. With the increase in the PCBM concentration in the polymer/PCBM film from the weight ratio of 1 : 2 to 1 : 3, V_{oc} and I_{sc} of the PSCs increased obviously, and so η increased, as shown in Table III. The positive effect of the PCBM concentration should have benefited from the larger interface areas of the donor (conjugated polymer)/acceptor (PCBM), and better acceptor networks formed in the photosensitive films with the increase in the PCBM concentration.[28] With a further increase in the PCBM concentration to the weight ratio of 1 : 4, I_{sc} decreased seriously, and V_{oc} also decreased a little. The phenomenon of V_{oc} decreasing with an increase in the PCBM concentration was also observed in other donor–acceptor systems.[29] The performance decrease of the PSCs with too high a PCBM concentration could be due to the aggregation of PCBM and poorer hole mobility in the blend films.[30]

CONCLUSIONS

A copolymer of dendronized PPV, BE-*co*-MEH–PPV, was synthesized with the Gilch route to improve the EL and photovoltaic properties of the dendronized PPV homopolymer. The polymer was characterized with UV–vis absorption spectroscopy, PL spectroscopy, and electrochemical cyclic voltammetry and compared with the homopolymers BE–PPV and MEH–PPV. PLEDs based on the polymers with the configuration of ITO/PEDOT : PSS/polymer/Ca/Al were fabricated. The EL efficiency of BE-*co*-MEH–PPV reached 1.64 cd/A, which was much higher than that of BE–PPV (0.68 cd/A) and a little higher than that of MEH–PPV (1.59 cd/A). The maximum luminance of BE-*co*-MEH–PPV reached 3988 cd/m^2 at 15 V, which was nearly 10 times that of BE–PPV. The photovoltaic properties of the polymer were studied with the device configuration of ITO/PEDOT : PSS/polymer : PCBM/Mg/Al. η of the device based on the blend of BE-*co*-MEH–PPV and PCBM with a weight ratio of 1 : 3 reached 1.41% under the illumination of AM1.5 (80 mW/cm^2), and this was also improved in comparison with 0.24% for BE–PPV and 1.32% for MEH–PPV under the same experimental conditions. These results indicate that BE-*co*-MEH–PPV is a promising EL and photovoltaic material.

TABLE III
Photovoltaic Properties of the PSCs Based on the Polymer/PCBM Blends

Active layer	I_{sc} (mA/cm^2)	V_{oc} (V)	FF (%)	η (%)
BE–PPV/PCBM (1 : 3)	0.63	0.75	41	0.24
BE-*co*-MEH–PPV/PCBM (1 : 2)	3.26	0.75	41	1.25
BE-*co*-MEH–PPV/PCBM (1 : 3)	3.37	0.81	42	1.41
BE-*co*-MEH–PPV/PCBM (1 : 4)	2.31	0.72	38	0.78
MEH–PPV/PCBM (1 : 3)	3.33	0.81	39	1.32

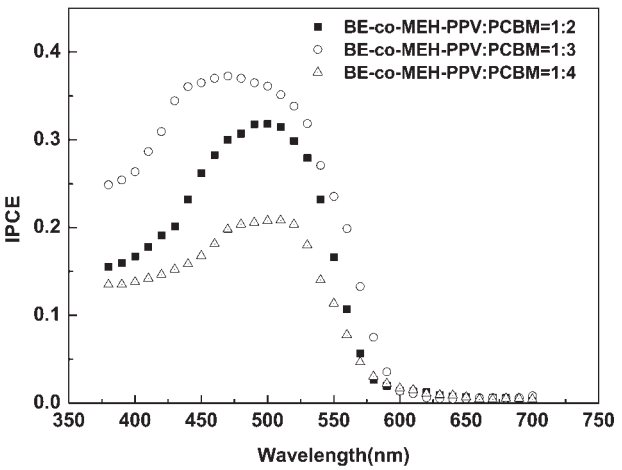

Figure 10 IPCE of the PSCs based on BE-*co*-MEH–PPV/PCBM.

References

1. Gustafsson, G.; Cao, Y.; Treacy, C. M.; Klavetter, F.; Colaneri, N.; Heeger, A. J. Nature 1992, 357, 477.
2. (a) Yang, C. H.; Sun, Q. J.; Qiao, J.; Li, Y. F. J Phys Chem B 2003, 107, 12981; (b) Tang, R. P.; Tan, Z. A.; Li, Y. F.; Xi, F. Chem Mater 2006, 18, 1053.
3. (a) Yu, G.; Gao, J.; Hummelen, J. C.; Wudl, F.; Heeger, A. J. Science 1995, 270, 1789; (b) Brabec, C. J. Sol Energy Mater Sol Cells 2004, 83, 273.
4. (a) Hou, J. H.; Tan, Z. A.; Yan, Y.; He, Y. J.; Yang, C. H.; Li, Y. F. J Am Chem Soc 2006, 128, 4911; (b) Halls, J. J.; Walsh, C. A.; Greenham, N. C.; Marseglia, E. A.; Friend, R. H.; Moratti, S. C.; Holmes, A. B. Nature 1995, 376, 498.
5. Shirringhaus, H.; Tessler, N.; Friend, R. H. Science 1998, 280, 1741.
6. (a) Hou, J. H.; Huo, L. J.; He, C.; Yang, C. H.; Li, Y. F. Macromolecules 2006, 39, 594; (b) Hou, J. H.; Yang, C. H.; He, C.; Li, Y. F. Chem Commun 2006, 871.
7. Spreitzer, H.; Becker, H.; Kluge, E.; Kreuder, W.; Schenk, H.; Demandt, R.; Schoo, H. Adv Mater 1998, 10, 1340.
8. Beek, W. J. E.; Wienk, M. M.; Janssen, R. A. J. Adv Mater 2004, 16, 1009.
9. Chu, H. Y.; Hwang, D. H.; Do, L. M.; Chang, J. H.; Shim, H. K.; Holmes, A. B.; Zyung, T. Synth Met 1999, 101, 216.
10. Hsieh, B. R.; Yu, Y.; Forsythe, E. W.; Schaaf, G. M.; Feld, W. A. J Am Chem Soc 1998, 120, 231.
11. Lee, S. H.; Jang, B. B.; Tsutsui, T. Chem Lett 2000, 11, 1184.
12. Peng, Z.; Zhang, J.; Xu, B. Macromolecules 1999, 32, 5162.
13. Tang, R. P.; Tan, Z. A.; Cheng, C. X.; Li, Y. F.; Xi, F. Polymer 2005, 46, 5341.
14. Tang, R. P.; Chuai, Y. T.; Cheng, Xi, C. X. F.; Zou, D. C. J Polym Sci Part A: Polym Chem 2005, 43, 3126.
15. Gilch, H. G.; Wheelwright, W. L. J Polym Sci Part A: Polym Chem 1966, 4, 1337.
16. Zeng, G.; Yu, W. L.; Chua, S. J.; Huang, W. Macromolecules 2002, 35, 6907.

17. Klärner, G.; Davey, M. H.; Chen, W. D.; Scott, J. C.; Miller, R. D. Adv Mater 1998, 10, 993.
18. Marsitzky, D.; Vestberg, R.; Blainey, P.; Tang, B. T.; Hawker, C. J.; Carter, K. R. J Am Chem Soc 2001, 123, 6965.
19. Hoppe, H.; Sariciftci, N. S. J Mater Res 2004, 19, 1924.
20. Hal, P. A. V.; Wienk, M. M.; Kroon, J. M.; Verhees, W. J. H.; Slooff, L. H.; Gennip, W. J. H. V.; Jonkheijm, P.; Janssen, R. A. J. Adv Mater 2003, 15, 118.
21. Wudl, F. G. U.S. Pat.5,189,136 (1993).
22. Li, Y. F.; Cao, Y.; Gao, J.; Wang, D. L.; Yu, G.; Heeger, A. J. Synth Met 1999, 99, 243.
23. Sun, Q. J.; Wang, H. Q.; Yang, C. H.; Li, Y. F. J Mater Chem 2003, 13, 800.
24. Precup-Blaga, F. S.; Garcia-Martinez, J. C.; Schenning, A. P. P. H. J.; Meijer, E. W. J Am Chem Soc 2003, 125, 12953.
25. Kwon, T. W.; Alam, M. M.; Jenekhe, S. A. Chem Mater 2004, 16, 4657.
26. Zhang, F. L.; Johansson, M.; Andersson, M. R.; Hummelen, J. C.; Inganas, O. Synth Met 2003, 137, 1401.
27. Alem, S.; de Bettignies, R.; Nunzi, J.-M.; Cariou, M. Appl Phys Lett 2004, 84, 2178.
28. Sariciftci, N. S.; Smilowitz, L.; Heeger, A. J.; Wudl, F. Science 1992, 258, 1474.
29. Chamberlain, G. A. Solar Cells 1983, 8, 47.
30. Mihailetchi, V. D.; Koster, L. J. A.; Blom, P. W. M.; Melzer, C.; de Boer, B.; van Duren, J. K. J.; Janssen, R. A. J. Adv Funct Mater 2005, 15, 795.